

Research Article

Cite this article: Ailán-Choke LG, Tavares LER, Luque JL, Pereira FB (2020). An integrative approach assesses the intraspecific variations of *Procamallanus (Spirocamallanus) inopinatus*, a common parasite in Neotropical freshwater fishes, and the phylogenetic patterns of Camallanidae. *Parasitology* **147**, 1752–1764. <https://doi.org/10.1017/S0031182020001687>

Received: 30 June 2020

Revised: 7 September 2020

Accepted: 8 September 2020

First published online: 14 September 2020


Key words:

Anostomidae; Characiformes; endoparasite; helminth; integrative taxonomy; morphology; Nematoda; genetic characterization

Author for correspondence:

Prof. Dr Felipe Bisaggio Pereira,
E-mail: felipebisaggio@hotmail.com

An integrative approach assesses the intraspecific variations of *Procamallanus (Spirocamallanus) inopinatus*, a common parasite in Neotropical freshwater fishes, and the phylogenetic patterns of Camallanidae

Lorena G. Ailán-Choke¹, Luiz E.R. Tavares², José L. Luque³
and Felipe B. Pereira⁴ 

¹Consejo Nacional de Investigaciones Científicas y Técnicas (CONICET), Instituto para el Estudio de la Biodiversidad de Invertebrados, Facultad de Ciencias Naturales, Universidad Nacional de Salta, Av. Bolivia 5150, (4400) Salta, Argentina; ²Departamento de Patologia, Instituto de Biotecnologia, Universidade Federal de Mato Grosso do Sul, Av. Costa e Silva s/n°, CEP 79070-900, Campo Grande, MS, Brasil; ³Departamento de Parasitologia Animal, Instituto de Veterinária, Universidade Federal Rural do Rio de Janeiro, BR 465, Km 47, CEP 23851-970, Seropédica, RJ, Brasil and ⁴Departamento de Parasitologia, Instituto de Ciências Biológicas, Universidade Federal de Minas Gerais, Av. Presidente Antônio Carlos, 6627, Pampulha, CEP 31270-901, Belo Horizonte, MG, Brasil

Abstract

Integrative taxonomy was used to evaluate two component populations of *Procamallanus (Spirocamallanus) inopinatus* in Brazil and the phylogeny Camallanidae. Parasite populations were collected in the characiform *Anostomoides passionis* from River Xingu (Amazon basin) and *Megaleporinus elongatus* from River Miranda (Paraguay basin). Morphology was analysed using light and scanning electron microscopy (SEM). Genetic characterization was based on partial sequences of the 18S and 28S rDNA, and COI mtDNA. Phylogenies were based on 18S and COI due to data availability. Generalized Mixed Yule Coalescent (GMYC), Poisson Tree Process (PTP) and *BEAST were used for species delimitation and validation. SEM revealed for the first time the presence of minute denticles and pore-like structures surrounding the oral opening, phasmids in females and confirmed other important morphological aspects. Statistical comparison between the two-component populations indicated morphometric variations, especially among males. The different component population of *P. (S.) inopinatus* showed variable morphometry, but uniform morphology and were validated as conspecific by the GMYC, PTP and *BEAST. Some camallanid sequences in GenBank have incorrect taxonomic labelling. Host, environment and geographic aspects seem to be related to some lineages within Camallanidae; however, their real phylogenetic meanings are still unclear.

Introduction

Procamallanus (Spirocamallanus) inopinatus Travassos, Artiga & Pereira, 1928 was originally described infecting the characiform fishes *Leporinus copelandii* Steindachner, 1855 and *Megaleporinus elongatus* (Valenciennes, 1850) from River Paraná Basin, Brazil (Travassos *et al.*, 1928; Kohn and Fernandes, 1987). Since then, the species has been reported in several families of Characiformes, Perciformes and Siluriformes, within a wide geographical range in South America including, besides Brazil, Argentina, Paraguay, Peru and Venezuela (see Moravec, 1998; Iannaccone *et al.*, 2000; Chemes and Takemoto, 2011; Luque *et al.*, 2011, 2016).

Due to its common occurrence, the general morphology of *P. (S.) inopinatus* has been well investigated suggesting that the species has homogenous morphology, but quite variable morphometry among component populations (Petter and Dlouhy, 1985; Kohn and Fernandes, 1987; Petter and Thatcher, 1988; Moravec *et al.*, 1993; 1997). Scanning electron microscopy (SEM) also has been used for observing the ultrastructure of *P. (S.) inopinatus*, but the detailing level was somewhat limited by the technology available at the time of such studies were performed (Moreira *et al.*, 1994; Moravec *et al.*, 1997). More recently, Vicentin *et al.* (2013) investigated *P. (S.) inopinatus* using SEM, but the approach of the study was not focused on the taxonomy of the species; therefore, results were not detailed.

Due to the lack of genetic data for *P. (S.) inopinatus*, its phylogenetic position within Camallanidae is unknown and the discussions regarding its wide morphometric variations among different populations remain without this important subsidy. Indeed, the phylogenetic aspects of Camallanidae are far from being elucidated due to the lack of genetic data, which is aggravated by the fact that the morphology-based systematics of the family is problematic and taxonomic labelling of some sequences available in genetic databases (e.g. GenBank) seems to be inaccurate (Černotíková *et al.*, 2011; Sardella *et al.*, 2017; Ailán-Choke *et al.*, 2019).

Therefore, the present study aimed to compare component populations of *P. (S.) inopinatus* from two different host species and localities using an integrative taxonomic approach and

evaluate the phylogenetic aspects of Camallanidae based on different computational tools (e.g. digital imaging, biostatistics, phylogenetic and species delimitation).

Materials and methods

Sampling and processing of hosts and nematodes

Hosts were sampled as follows: 10 specimens of *Anostomoides passionis* Santos & Zuanon, 2006 (Characiformes: Anostomidae) from River Xingu (RX), municipality of Altamira, State of Pará, Brazil (3°14'S; 52°06'W) in April 2013, and 12 specimens of *M. elongatus* (Anostomidae) from River Miranda (RM), municipality of Corumbá, State of Mato Grosso do Sul, Brazil (19°28'S, 57°02'W) in August 2018. Fish were kept alive in small water tanks with oxygen pumps until necropsy, through a ventral longitudinal incision from anus to operculum and extraction of the digestive tract. Organs (oesophagus, stomach, caeca, intestine) were placed individually in Petri dishes with saline and analysed using a stereomicroscope.

Nematodes were found alive, washed in saline, fixed in hot 4% formaldehyde solution and preserved in 70% ethanol. For morphological observations, nematodes were cleared in glycerine. One male of each infrapopulation (i.e. from each infected fish, see also Bush *et al.*, 1997 for details) had the mid-body excised and fixed in molecular-grade 96–99% ethanol for genetic studies; anterior and posterior parts were fixed for morphological identification.

Nomenclature and classification of hosts were updated following Froese and Pauly (2019), Frost (2020) and Uetz *et al.* (2020).

Morphological procedures

Nematodes were cleared in glycerine and observed in a Leica DM5500 B microscope, with DIC and the software LAS Leica™, for morphometric analysis. Measurements are given in micrometres unless otherwise stated. Specimens used for SEM (1 male and 1 female of each infrapopulation) were dehydrated through a graded ethanol series, dried by evaporation with hexamethyldisilazane, coated with gold and observed in a JEOL JSM 6460-LV, at an accelerating voltage of 15 kV. The systematic classification of camallanid nematodes follows the proposal of Moravec and Thatcher (1997). Voucher specimens were deposited in the Coleção Helmintológica do

Instituto Oswaldo Cruz (accession nos. CHIOC 38939, 38940).

Statistical analysis of morphological data

In order to evaluate significant differences among morphometric features, we performed a series of statistical analyses. First, one sample Kolmogorov–Smirnov (K-S) test was performed to verify the normal distribution of the quantitative variables (Zar, 2010). The quantitative variables were the standard length (SL) of fishes, and total body length, maximum width, buccal capsule length and width, distance from the anterior end to nerve ring, deirids and excretory pore, total length of oesophagus, tail length, distance from cephalic end to vulva in females and spicules in males of parasites. All these measurements were also used for calculating their ratio to total body length; the coefficient of variation (CV) for each of the previously mentioned features was also calculated. These morphometric features were chosen because they are used in the specific diagnosis, and ratios were used for verifying if the organ's anatomy (or their locations on the cuticle surface) undergoes modifications according to the parasite growth. Ratios and CV are expressed in percentage (%) and mean values are followed by ± 1 standard deviation unless otherwise stated.

According to the results of K-S test, we performed non-parametric inferential methods and generalized linear models (GLM). As a preliminary analysis, in order to verify possible influences of host-environment attributes and infection burden on the parasite body length, host SL and parasite intensity of infection (see Bush *et al.*, 1997) were tested as predictive of parasite body length using linear regression (Zar, 2010). First, host SL and parasite intensity of infection were tested separately against parasite body length using simple linear regression, in order to evaluate which variable was most predictive through the r^2 (coefficient of determination). Then a multiple linear regression was performed, inserting the predictive variables into the expected predictive model, in which the most predictive was inserted first followed by the less predictive (Zar, 2010). Following the previous methodology, but using logistic regression instead of linear, we tested the effect of host species and parasite sexual maturation (i.e. male, non-gravid and gravid females) on parasite body length, estimating the odds ratio (OR, $0 < OR < 1$ indicates antagonistic effect; OR = 1 lack of effect; OR > 1 synergetic effect) and the confidence interval (CI) of each model (Dohoo *et al.*, 2003). We also performed a Mann–Whitney (*U*) to evaluate and prove the differences in SL among the two fish species (Zar, 2010).

Following the preliminary analysis, parasites were divided into three categories according to sexual maturation: males, non-gravid females (without larvae in uterus) and gravid females (uterus filled with larvae). All morphometric features previously stated for parasites were tested against their total body length using the Spearman's correlation (r_s) (Zar, 2010), considering all sexual maturation categories. Differences in morphometric features of parasites among the two-component populations, i.e. from *A. passionis* and *M. elongatus*, were evaluated using the *U* test, within each sexual maturation category and among non-gravid and gravid females (Zar, 2010). Additional terminology related to parasite ecology follows the proposal of Bush *et al.* (1997).

Genetic procedures

Genomic DNA was isolated using DNeasy Blood & Tissue Kit (QIAGEN, Hilden, Germany), following the manufacturer's instructions. Three genetic regions were amplified: the 5' end of the 18S nuclear rDNA, the D2 and D3 domains of the nuclear 28S rDNA and the COI of the mtDNA. All polymerase chain reactions (PCRs), cycling conditions and primers are detailed in online Supplementary Material 1. PCR products were purified through an enzymatic treatment with ExoProStar™ (GE Healthcare) and sent for sequencing at ACTGene (Ludwig Biotec, Rio Grande do Sul, Brazil) with the same primers used in PCRs.

Contiguous sequences were assembled in Geneious (Geneious ver. 9.1.5 created by Biomatters, available from <http://www.geneious.com/>) and deposited in the GenBank. Preliminary BLAST search on GenBank database (<https://www.ncbi.nlm.nih.gov/genbank/>) was performed to confirm the genetic proximity between the present sequences and those from representatives of Camallanidae.

Phylogenetic analyses of molecular data

The phylogenetic reconstructions were based on three different datasets: with sequences of the 18S rDNA, with those of COI mtDNA and with sequences of 18S and COI concatenated. Due to the small number of sequences of the 28S rDNA and the high frequency of genetic gaps after aligning them, phylogenies based on this genetic region were not reconstructed; we used this genetic marker only for comparisons between the present samples. Sequences were chosen according to the following criteria: genetic regions congruent with those obtained in the present study and minimum length of 744 bp and 355 bp for 18S and COI, respectively (for details see Table 1).

Table 1. Species whose sequences were obtained from GenBank and used in phylogenetic reconstructions, associated with their hosts (habitat: Freshwater [FW] or Marine [MA]), geographic origin, accession number and genetic regions.

Parasite species	Host (habitat)	Geographic origin	18S	COI
<i>Batrachocamallanus slomei</i> ^a	<i>Xenopus laevis</i> (FW)	South Africa	–	MG948463
<i>Batrachocamallanus xenopodis</i>	<i>Xenopus muelleri</i> (FW)	South Africa	–	MN523681
<i>Camallanus cotti</i>	<i>Lentipes concolor</i> (FW) ¹ ; <i>Awaous guamensis</i> (FW) ² ; <i>Opsariichthys bidens</i> (FW) ³ ; <i>Odontobutis obscurus</i> (FW) ⁴	New Caledonia ² ; China ^{3, 4} ; India ⁵	EF180071 ¹ ; DQ442662 ² ; GU082507 ⁵	EU598879 ³ ; EU598876 ⁴ ; EU598845 ⁴ ; EU598833 ⁴ ;
<i>Camallanus hypophthalmichthys</i>	<i>Aristichthys nobilis</i> (FW) ¹	China ¹	JF803915 ¹	EU598816
<i>Camallanus kaapstaadi</i>	<i>Xenopus laevis</i> (FW)	South Africa	–	MG948461
<i>Camallanus lacustris</i>	<i>Sander lucioperca</i> (FW)	Czech Republic	DQ442663	–
<i>Camallanus oxycephalus</i>	<i>Lepomis</i> sp. (FW) ¹	India ²	DQ503463 ¹ ; GU082496 ² ; GU082497 ² ; GU170847 ² ; GU170848 ² ; GU170849 ² ;	–
<i>Camallanus xenopodis</i>	<i>Xenopus laevis</i> (FW)	South Africa	–	MG948462
<i>Paracamallanus cyathopharynx</i>	<i>Clarias gariepinus</i> (FW)	South Africa	–	MN523683
<i>Procamallanus</i> (P.) <i>annulatus</i>	<i>Siganus lineatus</i> (MAR)	New Caledonia	JF803932	–
<i>Procamallanus</i> (P.) <i>laeviconchus</i>	<i>Synodontis schall</i> (FW)	Sudan	JF803934	–
<i>Procamallanus</i> (P.) <i>pacificus</i>	<i>Anguilla obscura</i> (FW)	New Caledonia	DQ442665	–
<i>Procamallanus</i> (P.) <i>pseudolaeviconchus</i>	<i>Clarias gariepinus</i> (FW)	South Africa	–	MN523682
<i>Procamallanus</i> (P.) <i>sigani</i>	<i>Siganus fuscescens</i> (MAR)	China	HM545908	–
<i>Procamallanus</i> (P.) <i>spiculogubernaculus</i>	<i>Heteropneustes fossilis</i> (FW)	India	KU292357	KU292358
<i>Procamallanus</i> (S.) <i>fulvidraconis</i>	<i>Pelteobagrus fulvidraco</i> (FW) ^{1, 2}	China ^{1,2}	JF803914 ¹ ; DQ076689 ²	–
<i>Procamallanus</i> (S.) <i>huacraensis</i>	<i>Trichomycterus spegazzinii</i> (FW)	Argentina	MK794615	MK780067
<i>Procamallanus</i> (S.) <i>istiblenni</i>	<i>Lutjanus fulvus</i> (MAR) ¹ ; <i>Lutjanus kasmira</i> (MAR) ²	Hawaii ² ; India ³	EF180076 ¹ ; KC505629 ² ; KC505630 ² ; GU082491 ³ ; GU082492 ³ ; GU082493 ³ ; GU082495 ³ ; GU170858 ³	KC517382 ² ; KC517383 ²
<i>Procamallanus</i> (S.) <i>macaensis</i>	<i>Paralonchurus brasiliensis</i> (MAR)	Brazil	KY436826	–
<i>Procamallanus</i> (S.) <i>monotaxis</i>	<i>Lethrinus genivittatus</i> (MAR)	New Caledonia	JF803931	–
<i>Procamallanus</i> (S.) <i>philippinensis</i> ^b	<i>Siganus guttatus</i> (MAR)	Philippines	JF934736	–
<i>Procamallanus</i> (S.) <i>pintoii</i>	<i>Corydoras atropersonatus</i> (FW)	Peru	DQ442666	–
<i>Procamallanus</i> (S.) <i>rarus</i>	<i>Aguarunichthys</i> cf. <i>tocantinsensis</i> (FW) ¹ ; <i>Callophysus macropterus</i> (FW) ²	Peru ^{1, 2}	DQ494195 ¹ ; JF803912 ²	–
<i>Procamallanus</i> (S.) <i>rebecae</i>	<i>Cichlasoma meeki</i> (FW)	Mexico	DQ442667	–
<i>Serpinema cayennensis</i>	<i>Rhinoclemmys punctularia</i> (FW)	French Guiana	–	MN104841
<i>Spirocerca lupi</i> ^c	–	–	AY751497	MH633995

^aReferred as *Procamallanus slomei* in GenBank^bConsidered taxon inquirendum according to Horton *et al.* (2020)^cUsed as outgroup.

The 18S refers to the rRNA gene and the COI to the cytochrome c oxidase subunit I mtDNA. Superscript numbers make correspondence between information.

Sequences from samples not identified to species level and clones were excluded. We tried to use as many representatives as possible, including different samples from the same species for species delimitation and validation analyses. The outgroup was chosen according to previous phylogenies of Camallanidae (see Černotíková *et al.*, 2011). Sequences were aligned using M-Coffee (Notredame *et al.*, 2000), then evaluated by the transitive consistency score, to verify the reliability of aligned positions and, based on score values, ambiguously aligned positions were trimmed (Chang *et al.*, 2014). Saturation of nucleotide substitution was tested using Xia's method implemented in DAMBE (Xia *et al.*, 2003; Xia, 2018).

Datasets were subjected to maximum likelihood (ML) and Bayesian inference (BI) analyses, using PHYML and MrBayes, respectively (Huelsenbeck and Ronquist, 2001; Guindon and Gascuel, 2003). The model of evolution (nucleotide substitution) and its fixed parameters for each dataset were chosen and estimated under the Akaike information criterion with jModelTest 2 (Guindon and Gascuel, 2003; Darriba *et al.*, 2012); in the dataset of 18S + COI the partitions were treated separately and substitution models unlinked (see details in online Supplementary Material 2). Nodal supports for ML were based on 1000 bootstrap non-parametric replications. The same, but for BI posterior probability, were determined after running the Markov chain Monte Carlo (MCMC) (2 runs 4 chains) for 4×10^6 generations, with sampling frequency every 4×10^3 generations and discarding the initial $\frac{1}{4}$ of sampled trees (1×10^6) as burn-in. In order to check chain convergence, analyses were run in duplicates and inspected using Tracer (Rambaut *et al.*, 2018).

The genetic markers profile of phylogenetic informativeness was evaluated by PhyDesign (Townsend, 2007) based on the concatenated dataset (18S + COI). For this analysis, an ultrametric tree was generated using BEAST 2.5 (Bouckaert *et al.*, 2019), the best-fit substitution model was chosen according to bModelTest (Bouckaert and Drummond, 2017), models of each partition were unlinked, clock model was selected based on marginal likelihood estimated (MLE) from stepping stone and path sampling (Baele *et al.*, 2012) being 50 path steps, 5×10^5 iterations and sampling every 500 generations. MCMC chains were run for 5×10^7 generations, sampling every 5×10^3 generations and $\frac{1}{4}$ of initial runs discarded as burn-in. All analyses were run in duplicates and inspected with Tracer to check convergence. More information can be found in online Supplementary Material 2.

Species delimitation

We tested species hypotheses within Camallanidae mainly focused on the present samples. Two different species discovery methods and one species validation method were used to delimit species boundaries. Some analyses required ultrametric trees; these were generated in BEAST 2.5 as previously described and additional details are also in online Supplementary Material 2.

For species discovery, we used the Generalized Mixed Yule Coalescent (GMYC) method and the Poisson Tree Process (PTP) method, which do not require *a priori* assignments regarding putative species (Pons *et al.*, 2006; Zhang *et al.*, 2013). The GMYC requires an ultrametric guide tree, uses ML to delimit species and estimates a transition point before which all nodes reflects species diversification events and after which all nodes represent population-coalescent process (Pons *et al.*, 2006; Razkin *et al.*, 2016). GMYC tests were run in the webserver (<http://species.h-its.org/gmyc>) under the single-threshold and multiple-threshold models, for each dataset. The PTP does not require ultrametric trees; therefore, the major consensus tree generated from BI of each dataset was used in the analysis; this method tried to identify significant changes in the rate branching of the phylogenetic tree, using the number of substitutions. These

analyses were run in the bPTP webserver (<http://species.h-its.org/ptp>) using the default settings (1×10^5 generations, thinning set to 100, burn-in 1×10^4), which are adequate for datasets with < 50 taxa according to Zhang *et al.* (2013). PTP run both ML and BI to support the delimited species.

To validate the species, we used *BEAST (Heled and Drummond, 2010) implemented in BEAST 2.5 to generate unrooted (in order to improve species delimitation results; see Zhang *et al.*, 2013) species trees based on each dataset (minus outgroup sequences). *BEAST uses BI approach to generate phylogenies. We considered samples from the same species as different populations since they are mostly originating from different host individuals (see Table 1). Substitution models were chosen based on bModelTest, molecular clock selected based on MLE from stepping stone and path sampling, Yule process species tree priors and a constant root population size model. MCMC chains were run for 1×10^8 generations, sampling every 2×10^3 generations and $\frac{1}{4}$ of initial runs discarded as burn-in. Chains were run in duplicates and inspected with Tracer to check convergence. More information can be found in online Supplementary Material 2.

We also used the Automatic Barcode Gap Discovery (ABGD) method (Puillandre *et al.*, 2012) to generate pairwise (patristic) distance (*P*) matrixes, and thus evaluate intra and interspecific divergences among samples according to each genetic marker. The ABGD analyses were run online (<http://wwwabi.snv.jussieu.fr/public/abgd/>) using Kimura two-parameter (K2P) (Kimura, 1980) as the distance metric, with other parameters set to default. We refrain from the account the partitions generated by ABGD since intraspecific divergence of 18S and COI are poorly known and editing ABGD parameters for intraspecific genetic distance would generate mistaken results.

Results

The prevalence of *P. (S.) inopinatus* found in the present study was 30% (3 parasitized/10 examined) in *A. passionis* and 25% (3/12) in *M. elongatus*. The mean intensity of infection was 7.3 ± 1.5 (ranging from 6 to 9 parasites per infected host) in *A. passionis* and 8.0 ± 2.6 (0–11 per analysed host) in *M. elongatus*. Therefore, there were two-component populations (one from each host/locality) each composed of three infrapopulations of the parasite. *Procamallanus (S.) inopinatus* component population in *A. passionis* from RX had 9 males, 6 non-gravid and 7 gravid females; that in *M. elongatus* form RM had 11 males, 5 non-gravid and 8 gravid females. No concurrent infections were observed (i.e. the only helminth found was *P. (S.) inopinatus*). Specimens of *M. elongatus* were larger (SL 35.4 ± 1.3 cm; range 34.5–37.3 cm) than those of *A. passionis* (23.9 ± 1.2 cm; 23–25.5 cm); this difference was statistically significant ($p < 0.001$). The GLMs indicated no significant effect of host species ($P > 0.78$), SL ($P > 0.37$) and parasite intensity of infection ($P > 0.59$) in parasite body length. However, there was significant effect in parasite body length by sexual maturation ($P < 0.001$), in which males predicted smaller body length (OR = 0.687; CI 0.599–0.721), non-gravid females intermediate body length (OR = 1.233; CI 1.014–2.357) and gravid females larger body lengths (OR = 3.542; CI 2.987–3.881).

The following diagnostic features were constant and observed in the present specimens using SEM: cephalic end with two median teeth (one dorsal and one ventral) (Fig. 1A, B, online Supplementary Material 3), males with 10 pairs of subventral and sessile caudal papillae (4 pairs pre and 6 pairs proctocloacal) (Fig. 1E, F) and females without distinct terminal appendix on the tail (Fig. 1G, H). Also based on SEM observations, the presence of 6 pore-like structures (2 subdorsal, 2 subventral and 2 lateral) and of small pointed denticles surrounding the oral opening

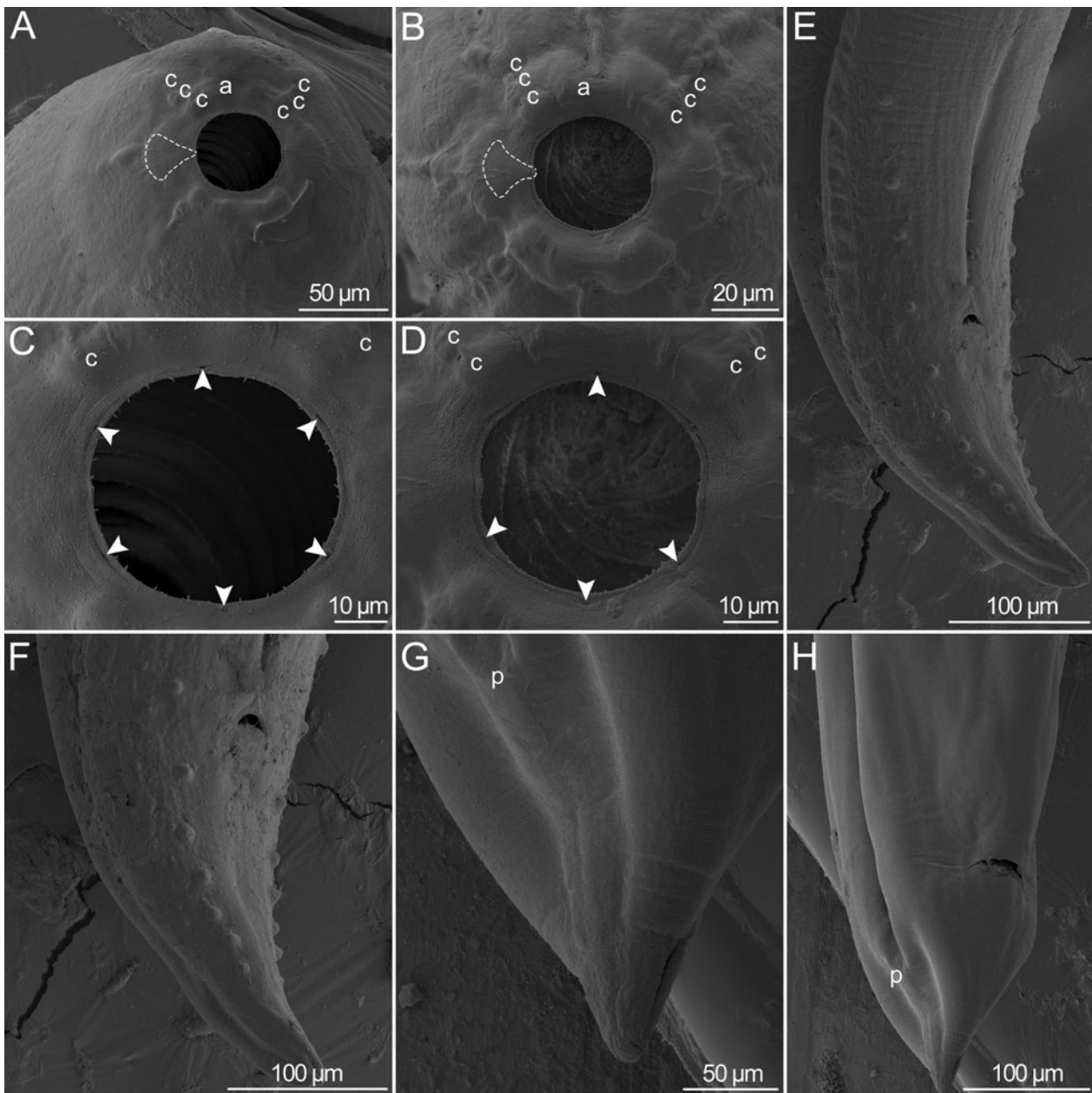


Fig. 1. *Procammallanus* (*Spirocamallanus*) *inopinatus*, ex. *Anostomoides passionis* (A, C, G, H) and *Megaleporinus elongates* (B, D, E, F), SEM micrographs **A, B:** Cephalic end of female and male, respectively, apical view (dashed lines delimit oral teeth). **C, D:** Oral opening of female and male, respectively (arrowheads indicate pore-like structures). **E, F:** posterior end and tail of male, respectively, sublateral views. **G, H:** tail and posterior end of female, respectively, sublateral views.

(Fig. 1A–D), as well as the phasmids of females (Figs 1G, H) are reported for the first time. The morphometric variations of the present specimens were within the range reported in previous studies. For these comparative measurements, as well as information on the host and locality of these studies see online Supplementary Material 4.

Most morphometric features of the present parasite specimens showed CV < 15%, with exception of some measurements related to deirids, excretory pore, tail and distance from the anterior end to vulva in females (see online Supplementary Material 5). The only CV higher than 20%, were observed in the ratio of the excretory pore to total body length (CV = 26.3%) and in the distance of vulva from the anterior end (CV = 24.3%), in gravid females from *A. passionis* (online Supplementary Material 4). Most morphometric features were correlated with a total body length of the parasites showing moderate to strong association (r^2 ranging from |0.594| to |0.928|), except by the length of tail ($P = 0.07$), length of spicules ($P = 0.6$), distance of vulva from anterior end

($P = 0.9$) and its relative position ($P = 0.1$) in females (online Supplementary Material 5). The size of all anatomic structures (except those previously mentioned) showed a positive correlation with a total body length; conversely, their ratios to total body length were negatively correlated, with exception of that of spicule (online Supplementary Material 5). Gravid females were larger and wider than those non-gravid (both $P < 0.001$), the tail to body length ratio was higher in non-gravid ($P < 0.001$) and vulva was more posterior in gravid specimens ($P = 0.01$); however, the relative position of vulva was similar in both gravid and non-gravid females ($P = 0.2$) (Table 2, online Supplementary Material 5). Width of buccal capsule and length of oesophagus were also higher in gravid females ($P = 0.014$ and < 0.001 , respectively); distance from the anterior end to deirid and nerve ring to total body length ratio also showed statistical differences according to female ontogeny (Table 2, online Supplementary Material 5).

Comparing the two-component populations of *P. (S.) inopinatus*, based on morphometry and according to sex and female

Table 2. Comparative measurements of *Procamallanus (Spirocamallanus) inopinatus* in the present study, according to host and locality.

Host Locality	<i>Anostomoides passionis</i>			<i>Megaleporinus elongatus</i>		
	River Xingu			River Miranda		
Specimens	Male (n = 9)	Gravid female (n = 7)	Non-gravid female (n = 6)	Male (n = 11)	Gravid female (n = 8)	Non-gravid female (n = 5)
Body length (mm)	6.87–7.57 ^a	20.38–31.00 ^b	15.25–18.32 ^c	5.23–7.78 ^a	20.57–24.37 ^b	15.32–21.84 ^c
Maximum width	351–361 ^a	572–826 ^b	396–501 ^c	150–240 ^a	680–760 ^b	400–615 ^c
Buccal capsule ridges*	13	13–15	13	11–14	17	12–16
Buccal capsule length	95–104 ^a	113–127 ^c	117–122 ^c	68–91 ^b	113–142 ^c	119–137 ^c
Buccal capsule width	76–112 ^a	123–146 ^c	132–134 ^d	70–78 ^b	123–158 ^c	110–122 ^e
Muscular oesophagus length*	404–451	409–578	449–501	270–370	500–550	350–400
Glandular oesophagus length*	598–646	821–1,170	770–855	410–550	925–940	510–745
Muscular/glandular oesophagus length ratio (%)*	63–70	46–55	57–65	54–73	53–54	51–78
Total oesophagus length (mm)	1–1.1 ^a	1.23–1.75 ^c	1.23–1.34 ^d	0.71–0.92 ^b	1.43–1.44 ^c	0.91–1.13 ^e
Total oesophagus/body length ratio (%)	15.8–17.4 ^a	5.00–7.20 ^c	7.70–9.70 ^{c, d}	10.3–13.7 ^b	5.08–5.90 ^c	5.20–6.80 ^{c, e}
Nerve ring to anterior end	174–210 ^a	251–286 ^b	253–262 ^b	121–208 ^a	235–270 ^b	215–280 ^b
Nerve ring to anterior end/body length ratio (%)	2.5–3.0 ^a	0.8–1.2 ^b	1.4–1.7 ^c	1.7–3.1 ^a	0.9–1.0 ^b	1.1–1.7 ^c
Deirids to anterior end	113–145 ^a	136–158 ^b	141–146 ^b	107–130 ^a	140–252 ^b	139–145 ^b
Deirids to anterior end/body length ratio (%)	1.6–1.9 ^a	0.5–0.7 ^b	0.8–0.9 ^c	1.6–2.1 ^a	0.6–1.0 ^b	0.6–0.9 ^c
Excretory pore to anterior end	310–430 ^a	368–485 ^c	387–476 ^{c, d}	182–260 ^b	340–390 ^c	280–400 ^{c, e}
Excretory pore to anterior end/body length ratio (%)	4.4–5.6 ^a	1.1–2.3 ^c	2.0–3.0 ^{c, d}	2.6–4.1 ^b	1.4–1.6 ^c	1.3–2.4 ^{c, d}
Spicule length	126–145 ^a	–	–	90–132 ^b	–	–
Spicule/body length ratio (%)	1.9–2.0 ^a	–	–	1.3–2.0 ^b	–	–
Vulva to anterior end (mm)	–	11.89–17.20 ^a	8.00–9.36 ^b	–	11.30–13.93 ^a	8.41–12.04 ^b
Relative position of vulva (%)	–	53.0–58.3 ^a	51.0–55.0 ^a	–	46.3–56.7 ^a	52.4–64.7 ^a
Tail length	291–322 ^a	180–200 ^a	180–187 ^a	168–268 ^b	180–210 ^a	160–280 ^a
Tail/body length ratio (%)	4.2–4.4 ^a	0.6–0.9 ^c	1.0–1.2 ^d	2.4–4.1 ^b	0.6–0.9 ^c	0.9–1.2 ^d

*Measurements not included in the statistical analysis.

Different superscript letters indicate measurements that showed statistical differences based on Mann-Whitney test, these comparisons are within each line of the table, respecting sexual maturation (for more information see online Supplementary Material 5).

ontogeny, most statistical divergences were observed among males. All measurements tended to be higher in males parasitizing *A. passionis*; however, the significance comparing the body length was in the borderline (i.e., $P = 0.05$) and the significant differences were found in buccal capsule length ($P = 0.003$) and width ($P = 0.006$), in excretory pore location ($P = 0.03$), as well as in the length of oesophagus ($P = 0.003$), spicules ($P < 0.03$) and tail ($P = 0.003$) (Table 2, online Supplementary Material 4). No statistical differences were observed comparing the morphometry of gravid females from *A. passionis* and *M. elongatus*, and regarding the non-gravid specimens from *A. passionis* showed wider buccal capsule ($P = 0.01$), more posterior excretory pore ($P = 0.03$) and larger oesophagus ($P = 0.01$) (Table 2, online Supplementary Material 5).

After sequencing of the genetic regions, 18S (GenBank accession nos. MT901634; MT901635) and COI (MT898796; MT898796) showed no polymorphisms within samples of the same component population; therefore, we used only one representative of each component population for genetic analyses. Three different genotypes were found for the 28S (MT901636–MT901638), two from parasites of *A. passionis* and one

from *M. elongatus*, in which the genetic similarity among them was $> 98\%$ (sequence lengths were 870 bp, 874 bp and 876 bp).

The partial 18S fragments were 892 bp long and showed only one polymorphism in the position 640 (A/C) according to component populations; their genetic similarity was 99.89% and the patristic distance $P = 0.00116$. *Promacallanus (S.) pinto* (Kohn & Fernandes, 1988) in the freshwater catfish *Corydoras atropersonatus* Weitzman & Nijssen, 1970 from Peru (DQ442666), was most similar to the present samples (genetic of similarity 94.13% and $P = 0.0117$ when compared with those parasites of *M. elongatus*; genetic similarity of 94.24% and $P = 0.0105$ when compared with those parasites of *A. passionis*). The partial coding fragments of COI were 388 bp long, the genetic similarity among samples from *M. elongatus* and *A. passionis* was 90.72%, the patristic distance $P = 0.09901$ and no polymorphism resulted in amino acid residue change. These sequences were most similar to that of *P. (S.) istiblenni* (Noble, 1966) parasitizing the marine snapper *Lutjanus kasmira* (Forsskål, 1775) from Hawaii (KC517382) (genetic similarity 86.18% and $P = 0.1515$ from parasites of *M. elongatus* and 84.75% and $P = 0.1700$ from parasites of *A. passionis*). Genetic alignments showed no substantial nucleotide saturation (18S:

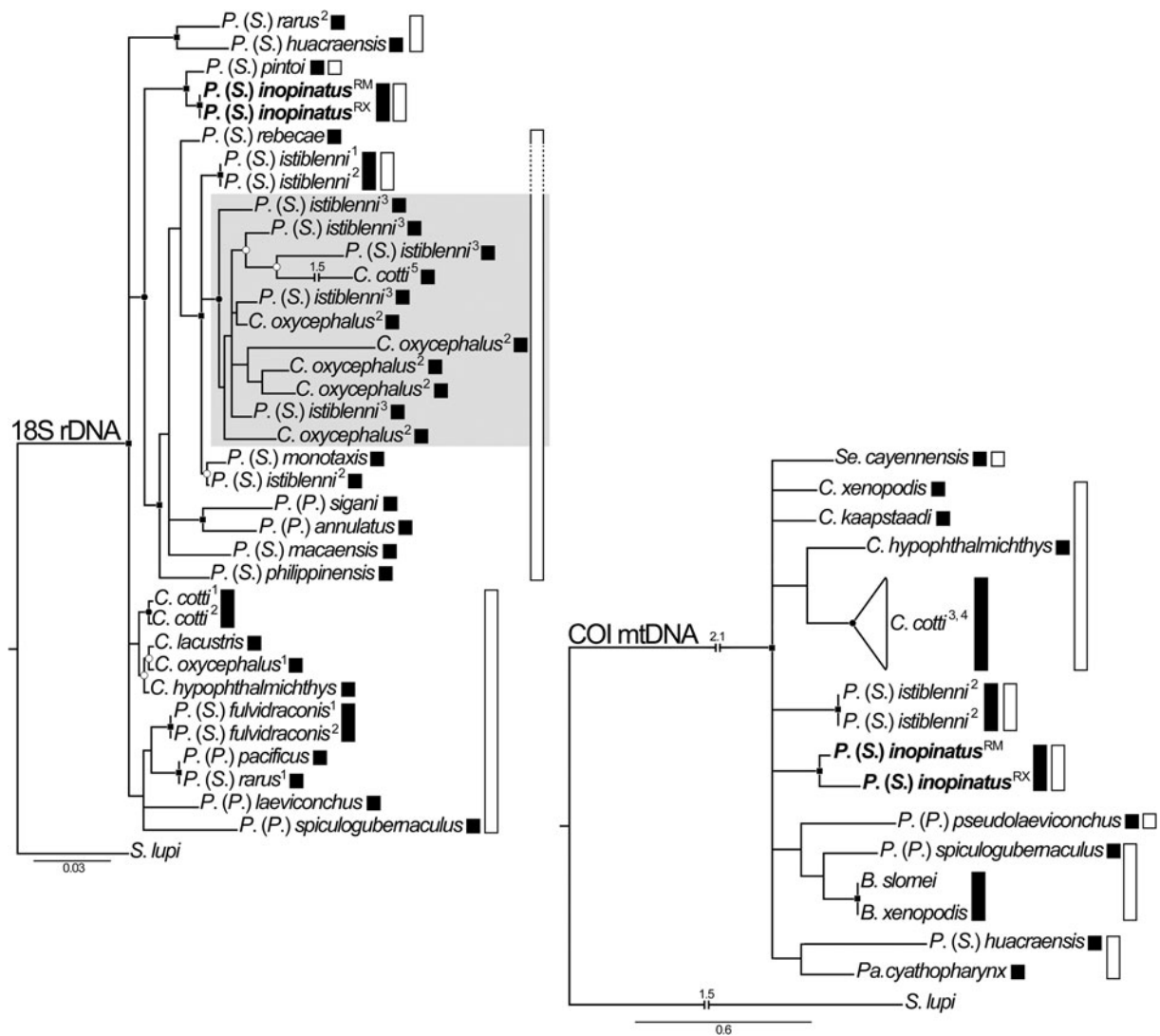


Fig. 2. Phylogenetic trees generated using Bayesian Inference from sequences of camallanid nematodes. Nodal supports are indicated on tree nodes, according to the Bayesian posterior probability (BPP) and maximum likelihood (ML) bootstrap replications as follows: full squares (BPP = 1, ML = 100%), full circles (0.96 < BPP < 1, 90% < ML < 100%) and empty circles (0.90 < BPP < 0.96, 95% < ML < 90%). Black polygons next to taxa labels indicate specific entities recognized by the Poisson Tree Process (PTP) and those white by the Generalized Mixed Yule Coalescent (GMYC); superscript numbers make correspondence with information in Table 1. The shaded clade represents atypical phylogenetic behaviour and includes sequences with apparently taxonomic misidentification. Sequences from the present study are in bold and superscriptions are RM = River Miranda, RX = River Xingu.

Iss = 0.068, Iss.c = 0.804, $P < 0.001$; COI: Iss = 0.2612, Iss.c = 0.6761, $P < 0.001$). BLAST search indicated that the representative from GenBank database most genetic similar to the present sequences was *C. xenopodis* Jackson & Tinsle, 1995 [MG947389] (genetic similarity of 64.4%).

The phylogenies using 18S sequences included more representative taxa than those using COI and 18S + COI, because of data availability (Table 1, Figs 2–4). The phylogenetic meaning of the trees reconstructed using ML and BI was the same; therefore, only BI trees were depicted. Monophyly of Camallanidae was strongly supported in all phylogenies (Figs 2, 3); in contrast, its genera and subgenera were not monophyletic (Figs 2, 4). A monophyletic assemblage including sequences with the same origin from India, shaded in the trees of the 18S, made the following species not monophyletic: *Camallanus cotti* Fujita, 1927, *C. oxycephalus* Ward & Magarh, 1917 and *P. (S.) istiblenni*. *Procamallanus (S.) rarus* Travassos, Artigas & Pereira, 1935 was also non-monophyletic and unrelated to the shaded clade (Figs 2, 4). Samples from the present study formed well-supported monophyletic assemblages in all the phylogenies (Figs 2–4). The phylogenetic informativeness of COI was better for analysing divergences and similarities among

inner nodes (e.g. closely related taxa, such as those species) and that of 18S better for evaluating divergence events related to more external nodes (e.g., for comparing genera) (Fig. 3).

Regarding the species delimitation analyses, PTP was more concordant with the molecular phylogenetic approach than GMYC (Figs 2, 3). ML of the GMYC was significantly higher than the null model, except for the 18S dataset (see online Supplementary Material 6). The entities recognized by the PTP model showed high support values for both ML and Bayesian approaches (see online Supplementary Material 6). The present samples were recognized as a single species by both methods, in all datasets (Figs 2, 3). In the tree of 18S sequences, PTP indicated that *P. (S.) istiblenni* represented 7 different specific entities, *C. oxycephalus* 6, *C. cotti* and *P. (S.) rarus* 2 each (Fig. 2). In the tree of COI sequences, PTP agreed with taxonomic labelling of all species, except *B. slomei* and *B. xenopodis* that were recognized as a single species (Fig. 2), and the K2P distance between these sequences (MG948463/ MN523681) was null ($P = 0$). The concordance of these methods (mainly PTP) with the taxonomic labelling of the sequences was higher in the dataset of COI and 18S + COI sequences, as expected (Figs 2, 3).

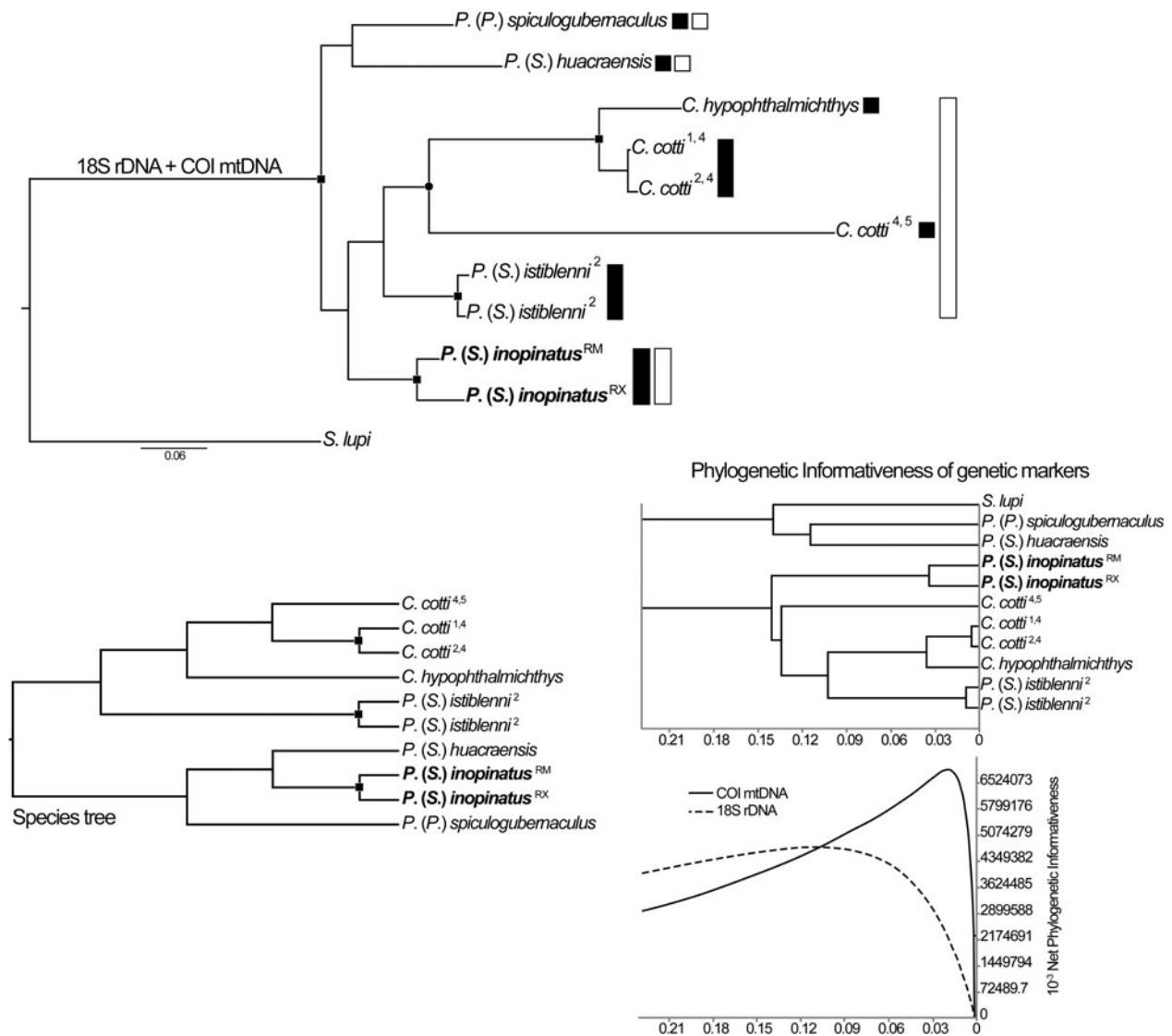


Fig. 3. Phylogenetic trees generated from concatenated sequences of the 18S rDNA and COI mtDNA of camallanid nematodes using Bayesian Inference. Upper centre tree is the output of Mr. Bayes (gene tree), bottom right is the output of PhyDesign (which does not estimate nodal supports) associated with graphical representation of phylogenetic informativeness for each generic marker, bottom left is a species tree output of *BEAST from 18S and COI concatenated. Nodal supports are indicated on tree nodes, according to the Bayesian posterior probability (BPP) and maximum likelihood (ML) bootstrap replications as follows: full squares (BPP = 1, ML = 100%), full circles (0.96 < BPP < 1, 90% < ML < 100%) and empty circles (0.90 < BPP < 0.96, 95% < ML < 90%). Black polygons next to taxa labels indicate specific entities recognized by the Poisson Tree Process (PTP) and those white by the Generalized Mixed Yule Coalescent (GMYC); superscript numbers make correspondence with information in Table 1. Sequences from the present study are in bold and superscriptions are RM = River Miranda, RX = River Xingu.

Species tree approach validated the results of phylogenetic and species delimitation methods (mainly of PTP) (Figs 2–4). Samples of *P. (S.) inopinatus* were validated as a single species, whereas those that appeared as non-monophyletic were not validated as single species, and, as same as in species delimitation approach, *B. slomei* and *B. xenopodis* and recognized as a single lineage; nodal supports in these cases were medium to high (Fig. 4). We indicated host, geographic origin and environmental features related to samples in the species tree of 18S and COI (Fig. 4). Thus, most phylogenetic assemblages did not show similarities regarding these characteristics, except the clade A in Fig. 4 that grouped species from freshwater hosts and the shaded one, composed of species from India, with no additional information. These clades showed average nodal supports (Fig. 4). It should be mentioned that *P. (S.) inopinatus* was phylogenetically close to samples isolated from freshwater fishes of the Neotropical region.

The pairwise distances between samples of *P. (S.) inopinatus* were $P = 0.001$ and $P = 0.099$ in 18S and COI matrices, respectively. Lower than these, were the distances between representative of *P. (S.) fulvidraconis* Li, 1935 (DQ076689/JF803914) and *P. (S.)*

istiblenni (EF180076/KC505629) (both $P = 0$) in 18S matrix, representatives of *C. cotti* (DQ442662/EU598876/EU598845; $P < 0.014$), *C. oxycephalus* (EU598879/EU598876/EU598833/EU598845; $P < 0.014$) of *P. (S.) istiblenni* (KC517382/KC517383; $P = 0.002$) and between *B. slomei* Southwell & Krishner, 1937 (MG948463) and *B. xenopodis* (MN523681) ($P = 0$) in COI matrix. Pairwise distances also corroborated previous phylogenetic, species delimitation and validation results, in which representatives of *C. cotti*, *C. oxycephalus* and *P. (S.) istiblenni* forming the shaded clade (Figs 2, 4) showed values of genetic distance relatively high ($P > 0.013$) when compared with their conspecifics placed out of this clade. Samples of *P. (S.) rarus* (DQ494195/JF803912) also showed similar results ($P = 0.048$). Complete distance matrices and comparative tables are available in online Supplementary Material 7, 8, 9.

Discussion

As previously commented, *Procamallanus (S.) inopinatus* is a nematode parasite with suggestively low host specificity and wide

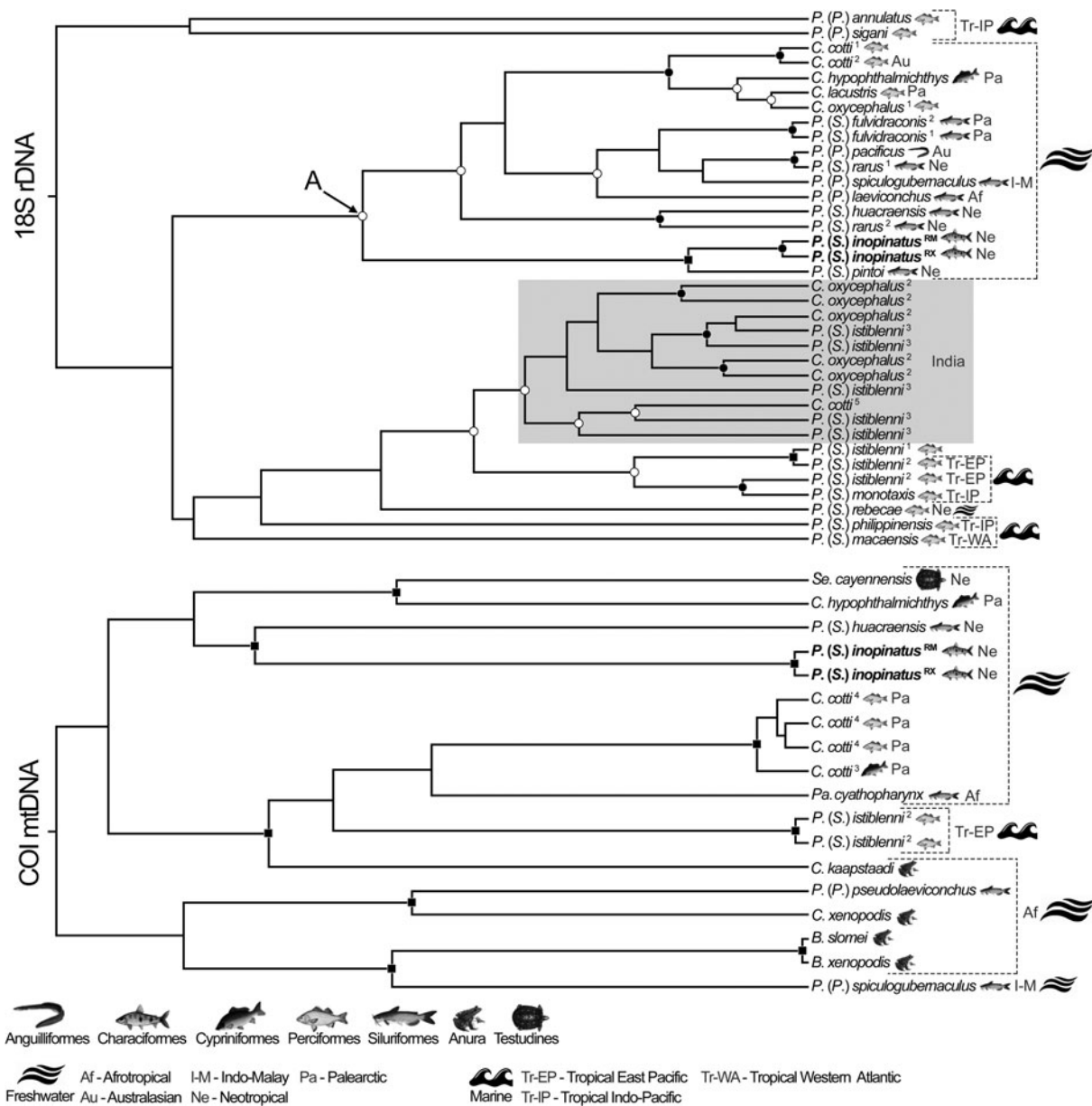


Fig. 4. Species trees based on 18S rDNA and COI mtDNA sequences of camallanid nematodes generated using *BEAST, for species validation. Nodal supports are indicated on tree nodes, according to the Bayesian posterior probability (BPP) as follows: full squares (BPP = 1), full circles (0.96 < BPP < 1) and empty circles (0.90 < BPP < 0.96). Superscript numbers make correspondence with information in Table 1. The shaded clade represents atypical phylogenetic behaviour and includes sequences with apparently taxonomic misidentification. Letter A highlights the clade formed exclusively by species from freshwater hosts. Order of hosts, geographic origin and environment associated with each sequence are depicted. Sequences from the present study are in bold and superscriptions are RM = River Miranda, RX = River Xingu.

distribution in the freshwaters of South America (from North to South-western Brazil, Venezuela, Peru and Argentina) (see Moravec, 1998; Chemes and Takemoto, 2011; Luque et al., 2011, 2016). Some aspects of its taxonomic assessment have been controversial, especially considering the spiral ridges in the buccal capsule (see Moravec et al., 1993, 1997). Despite the wide variation in the number of spiral ridges in *P. (S.) inopinatus* (13–23, see online Supplementary Material 4), they occupied no more than 2/3 of the buccal capsule as shown herein and in other studies (Travassos et al., 1928; Pereira, 1935; Kloss, 1966; Petter and Thatcher, 1988; Moravec et al., 1993, 1997; Abdallah et al., 2012). Reciprocally, Petter and Dlouhy (1985) described this structure completely occupied by the spiral ridges and Vicentin et al. (2013) reported the same characteristic but based only on female specimens; both studies analysed characiform fishes from River Paraguay basin (as in the present study). These observations indicate that this characteristic may be a rare intraspecific variation in

P. (S.) inopinatus. However, to confirm this assertion, specimens with the whole buccal capsule occupied by spiral ridges need to be genetically characterized and compared to the present data. It should be mentioned that, based on genetic evidence, the morphology of buccal capsule seems to bear some degree of artificiality in the systematics of genera and subgenera of Camallanidae (Wijová et al., 2006; Sardella et al., 2017; Ailán-Choke et al., 2019), which may be also true at the species level, as suggested here.

Moreira et al. (1994) performed the first observation of *P. (S.) inopinatus* using SEM and reported 3 circles of 4 cephalic papillae each in the species. Later, Moravec et al. (1997) described only 2 circles with 4 papillae each, also using SEM. Based on the present results it was possible to confirm the observations of Moreira et al. (1994) through higher resolution micrographs. The present observations also reported for the first time small denticles and pore-like structures surrounding the oral opening internally and externally, respectively. It should be mentioned that Vicentin

et al. (2013) reported only 1 circle of 4 cephalic papillae in *P. (S.) inopinatus*, which is a misinterpretation since in the SEM micrograph provided by the authors it is possible to observe the 2 additional circles of cephalic papillae (see Fig. 1A by Vicentin *et al.*, 2013). The presence of two large (dorsal and ventral) teeth (see Petter and Thatcher, 1988; Moreira *et al.*, 1994) was also confirmed and phasmids in female were observed for the first time, contributing to the morphological knowledge of *P. (S.) inopinatus*.

The present results showed that almost all measurements used for taxonomic diagnosis had a medium to strong correlation with the body length of parasites. Measurements of the organs showed a positive correlation (except the length of spicules and the distance from cephalic and to vulva) whereas the ratio of these measurements to total body length showed negative correlation (see online Supplementary Material 5). It indicates that the growth rates of body and organs are markedly different, in which the first grows much faster than the second (a matter of mathematic reason: if the divisor, i.e., body length, is much higher than the dividend, i.e., the measure of a given organ, the quotient will be low). Moreover, these results indicate general morphometric dependence on body length, except by the spicule length and the relative position of vulva, which are more constant and, consequently, more reliable for intraspecific comparisons, regardless of body length and sexual maturation of *P. (S.) inopinatus*.

Sexual maturation of females of *P. (S.) inopinatus* in the present study had a significant effect on their body length, in which gravid specimens were larger than the non-gravid. As a consequence, some ratio measurements, the maximum body and buccal capsule width, oesophagus length, distance from cephalic end to vulva, but not its relative position (vulva to body length ratio), were statistically different (Table 2, online Supplementary Material 5). Therefore, the morphometry of gravid and non-gravid females should be presented separately. However, several studies do not follow this proposal, making the morphometric range of females of *P. (S.) inopinatus* very wide (see online Supplementary Material 4). Male specimens are evidently smaller than females (present results showed males as predictive of smaller body length) and also exhibit the same wide morphometric ranges, comparing the present results with the previous studies (see online Supplementary Material 4). Thus, researchers should be aware when dealing with the morphometry of *P. (S.) inopinatus* and focus on morphology (see further discussion).

Despite the intensity of infection, host species and SL did not have an effect in the body length of the present parasites; the statistical comparison between specimens of the two-component populations evidenced the morphometric differences from males and non-gravid females, but not from those gravid. It indicates that, once these females reach full sexual maturity, their growth stabilizes (other argument supporting the assertion for separating measurements from non-gravid and gravid specimens). The main differences comparing non-gravid females and males from the two-component populations were in the position of excretory pore and in the length of oesophagus; these variations can be observed in *P. (S.) inopinatus* from different hosts and river basins (Petter and Dlouhy, 1985; Petter and Thatcher, 1988; Moravec *et al.*, 1993; 1997). Although the body length is similar between males from the present component populations, specimens parasitizing *A. passionis* showed larger spicules. The size of these structures is very important in the taxonomy of *Procamallanus (Spirocamallanus)* spp. (Moravec *et al.*, 2000; Moravec and Jirků, 2015; Pinheiro *et al.*, 2018; Moravec and Justine, 2019). However, in *P. (S.) inopinatus* the length of spicules seems to be random and not correlated with body length, some of the smallest males have average spicule length (e.g. Petter and Thatcher, 1988) whereas some of the larger specimens have

them short (e.g. Moravec *et al.*, 1997) (see also online Supplementary Material 4).

The present morphometric heterogeneity observed in *P. (S.) inopinatus* represents a phenotypic plasticity characteristic of the species, also observed in previous studies (see online Supplementary Material 4). Moreover, although the morphology of *P. (S.) inopinatus* is almost constant, the number and distribution of spiral ridges on its buccal capsule is highly variable. In fact, these features have been pointed out as weak taxonomic characters within the complicated systematics of Camallanidae (Wijová *et al.*, 2006; Černotíková *et al.*, 2011; Sardella *et al.*, 2017; Ailán-Choke *et al.*, 2019). Therefore, in order to avoid further taxonomic confusions, we suggest that the specific diagnosis of *P. (S.) inopinatus* should be based on the presence of two large (one dorsal and one ventral) oral teeth at the cephalic end, which represent the single autapomorphy of the species so far.

The present and first genetic characterization of *P. (S.) inopinatus* supported the results of morphological analysis, in which the morphology of the specimens was constant among the component populations. It also reaffirms the characteristic wide morphometric variation of the species. The pairwise distances of both 18S and COI among the present sequences were low, as same as observed between representatives of *C. cotti* (DQ442662/ EF180071 from 18S and EU598833/ EU598845 EU598876/ EU598879 from COI), *P. (S.) istiblenni* (KC505629/ KC505630 from 18S and KC517382/ KC517383) and *P. (S.) fulvidraconis* (DQ076689/ JF803914 from 18S) (for more details see online Supplementary Material 7, 8). The present 28S sequences also supported that the samples are conspecific; their genetic similarity was much higher than that of the most closely related sample from GenBank database (i.e. *C. xenopodis*). Unfortunately, 28S sequences from GenBank are currently very limited in number and length, giving no robustness for comparing the present intraspecific genetic variations with that from other species. Similarly, species delimitation and validation approaches indicated that *P. (S.) inopinatus* in *A. passionis* from River Xingu (Amazon basin) and in *M. elongatus* from River Miranda (Paraguay basin) are conspecific. It should be highlighted that GMYC was more conservative than PTP, regarding species delimitation and the accuracy of the methods was higher in the databases including COI (see online Supplementary Material 6), because this genetic region was more informative for analysing divergences and similarities among closely related taxa than the 18S (see Fig. 3); this is due to the fact that, in metazoans, mtDNA genes evolve at faster rates than those from nuclear DNA (Allio *et al.*, 2017).

The overall phylogeny of Camallanidae was poorly resolved and monophyly was not observed in most genera and subgenera as a consequence of the morphology-based systematics that predominantly uses the buccal capsule structure as a diagnostic feature, which seems to be artificial as commented previously (Wijová *et al.*, 2006; Černotíková *et al.*, 2011; Sardella *et al.*, 2017; Ailán-Choke *et al.*, 2019).

The genus *Batrachocamallanus* Jackson and Tinsle, 1995 is a particular case; it has been considered a synonym of *Procamallanus (Procamallanus)* Baylis, 1923 by some authors (Moravec *et al.*, 2006) and valid by others (Jackson and Tinsle, 1995; Svitin *et al.*, 2018; 2019). The buccal capsule structure in both taxa is the same and the characters used in the differential diagnosis of *Batrachocamallanus* were refuted and proved to be also present in *Procamallanus (Procamallanus)* (see Moravec *et al.*, 2006). Therefore, we agree with the proposal of Moravec *et al.* (2006) and consider *Batrachocamallanus* junior synonym of *Procamallanus (Procamallanus)*. In this sense, the present genetic analyses support the previous assertion because GMYC considered the two representatives, labelled *B. slomei* Southwell & Kirshner, 1937 and *B. xenopodis* (Baylis, 1929), along with

P. (P.) spiculocubernaculus Agarwal, 1958 as a single species and in the species tree they were closely related with full nodal support. Furthermore, sequences from *B. slomei* and *B. xenopodis* were 100% similar, but we will not assume their synonymy, since data represent only a small and partial fragment of a gene.

In the phylogenetic reconstructions using 18S sequences, representatives of *P. (S.) inopinatus* formed a fully supported assemblage with *P. (S.) pintoii*, which was also closely related to *P. (S.) rarus* and *P. (S.) huacraensis* Ramallo, 2008, all representatives isolated from freshwater catfishes, in the Amazon (the first two) and la Plata basin (the last). When COI sequences were included in the analysis, the phylogenetic position of *P. (S.) inopinatus* was somewhat uncertain, but not in the species tree that provides a better genealogy of taxa (Nichols, 2001) and where it formed a fully supported assemblage with *P. (S.) huacraensis*. The recent ancestry of the all previously mentioned species is probably the same (or closely related), since the geological and biogeographic history in South America, indicates the close relatedness between the Amazon la and Plata basins (which includes Paraná basin), and the tandem evolution of their fish fauna (Albert and Reis, 2011; Reis et al., 2016; Dagosta and Pinna, 2017). Moreover, *P. (S.) inopinatus* also parasitizes catfishes (see Moravec, 1998; Iannacone et al., 2000; Chemes and Takemoto, 2011; Luque et al., 2011, 2016). These relationships between habitat, host taxa, geographic origin and the phylogenetic aspects of camallanids cannot be generalized and are unclear, since as same as some assemblages were formed by samples isolated from freshwater hosts, they were from very different geographic origins and host taxa; other assemblages were formed independently from these characteristics. Similar results were previously observed (Wijová et al., 2006; Ailán-Choke et al., 2019).

The conspecific-labelled sequences referring to *C. cotti*, *C. oxycephalus*, *P. (S.) istiblenni* and *P. (S.) rarus* were not monophyletic. The main responsible for this result was the shaded clade in Figs 2, 4, composed by sequences with the same origin (location and authors), with poorly detailed information and unpublished in scientific papers. The usage of these sequences generated misleading results, which were kept here with the intent of highlighting the importance of a careful analysis when dealing with the genetic database of camallanids, since these data have considerable taxonomic inaccuracies also observed in other studies (Černotíková et al., 2011; Ailán-Choke et al., 2019).

The present approach confirmed that the general morphometry of *P. (S.) inopinatus* is markedly variable, whereas the general morphological features are constant, especially the following that should be used for species diagnosis: the presence of two large (dorsal and ventral) oral teeth (only synapomorphy of the species), the relative position of vulva (on the second third of body) and 10 then pairs of subventral caudal papillae in males (4 pairs pre and 6 pair post cloacal). The present genetic characterization and the phylogenetic analyses supported the morphological analyses and that the component populations of *P. (S.) inopinatus* from *A. passionis* and *M. elongatus* are conspecific, their genetic structure differ, but this difference is minimal regarding all genetic markers analysed. The data provided here improve the current scarce genetic database of camallanid nematodes and represents the first step for a better understanding of the genetic population structure of *P. (S.) inopinatus*.

Supplementary material. The supplementary material for this article can be found at <https://doi.org/10.1017/S0031182020001687>

Acknowledgements. The authors would like to thank Dr Elias Nogueira de Aguiar from the Laboratório Multiusuário de Análises de Materiais do Instituto de Física (MULTILAM-INF), Universidade Federal de Mato Grosso do Sul (UFMS), for help with scanning electron microscopical procedures. Dr Carina Elisei from the Universidade Católica Dom Bosco provided

the facilities for molecular studies. Dr Philippe Vieira Alves for valuable conversations that inspired the approach of the present manuscript and Lennon de Souza Malta for his assistance in field collections and laboratorial procedures.

Financial support. This work was financed in part by the Coordenação de Aperfeiçoamento de Pessoal de Nível Superior-Brasil (CAPES)-Finance code 001 and by the Conselho Nacional de Desenvolvimento Científico e Tecnológico – Brazil (Proc. 474077/2011-0).

Conflict of interest. None.

Ethical standards. All procedures involving animal manipulation were permitted by Sistema de Informação e Autorização em Biodiversidade (license number 54895) and were in strict accordance with the recommendations of the Colégio Brasileiro de Experimentação Animal.

References

- Abdallah VD, Azevedo RK, Carvalho ED and Silva RJ (2012) New hosts and distribution records for nematode parasites of freshwater fishes from São Paulo State, Brazil. *Neotropical Helminthology* **6**, 43–57.
- Ailán-Choke LG, Davies DA, Tavares LER and Pereira FB (2019) An integrative taxonomic assessment of *Procamallanus* (*Spirocamallanus*) *huacraensis* (Nematoda: camallanidae), infecting the freshwater catfish *Trichomycterus spegazzinii* (Siluriformes: Trichomycteridae) in Argentina. *Parasitology Research* **118**, 2819–2829.
- Albert JS and Reis RE (2011) *Historical Biogeography of Neotropical Freshwater Fishes*. Berkeley, CA: University of California Press.
- Allio R, Donega S, Galtier N and Nabholz B. (2017) Large variation in the ratio of mitochondrial to nuclear rate across animals: implications for genetic diversity and the use of mitochondrial DNA as a molecular marker. *Molecular Biology and Evolution* **34**, 2762–2772.
- Baele G, Li WS, Drummond AJ, Suchard MA and Lemey P (2012) Accurate model selection of relaxed molecular clocks in Bayesian phylogenetics. *Molecular Biology and Evolution* **30**, 239–243.
- Bouckaert R and Drummond A (2017) Bmodeltest: Bayesian phylogenetic site model averaging and model comparison. *BMC Evolutionary Biology* **17**, 42.
- Bouckaert R, Vaughan TG, Barido-Sottani J, Duchêne S, Fourment M, Gavryushkina A, Heled J, Jones G, Kühnert D, De Maio N, Matschiner M, Mendes FK, Müller NF, Ogilvie HA, du Plessis L, Popinga A, Rambaut A, Rasmussen D, Siveroni I, Suchard MA, Wu, C-H., Xie D, Zhang C, Stadler T and Drummond AJ (2019) BEAST 2.5: an advanced software platform for Bayesian evolutionary analysis. *PLoS Computational Biology* **15**, e1006650.
- Bush AO, Lafferty KD, Lotz JM, Shostak AW (1997) Parasitology meets ecology on its own terms: Margolis et al. revisited. *Journal of Parasitology* **83**, 575–583.
- Černotíková E, Horák A and Moravec F (2011) Phylogenetic relationships of some spirurine nematodes (Nematoda: Chromadorea: Rhabditida: Spirurina) parasitic in fishes inferred from SSU rRNA gene sequences. *Folia Parasitologica* **58**, 135–148.
- Chang, J-M, Di Tommaso P and Notredame C (2014) TCS: a new multiple sequence alignment reliability measure to estimate alignment accuracy and improve phylogenetic tree reconstruction. *Molecular Biology and Evolution* **31**, 1625–1637.
- Chemes SB and Takemoto RM (2011) Diversity of parasites from middle Paraná system freshwater fishes, Argentina. *International Journal of Biodiversity and Conservation* **3**, 249–266.
- Dagosta FCP and Pinna M (2017) Biogeography of Amazonian fishes: deconstructing river basins as biogeographic units. *Neotropical Ichthyology* **15**, e170034.
- Darriba D, Taboada GL, Doallo R and Posada D (2012) Jmodeltest 2: more models, new heuristics and parallel computing. *Nature Methods* **9**, 772.
- Dohoo I, Martin W and Stryhn H (2003) *Veterinary Epidemiologic Research*. Charlottetown: AVC Inc.
- Froese R and Pauly D (eds) (2019) FishBase. World Wide Web electronic publication. <http://www.fishbase.org> (accessed 25 May 2020).
- Frost DR (2020) Amphibian Species of the World: an Online Reference. Version 6.1. World Wide Web electronic publication. <https://amphibiansoftheworld.amnh.org/index.php>. (accessed 25 August 2020). doi.org/10.5531/db.vz.0001.
- Guindon S and Gascuel O (2003) A simple, fast, and accurate algorithm to estimate large phylogenies by maximum likelihood. *Systematic Biology* **52**, 696–704.
- Heled J and Drummond AJ (2010) Bayesian Inference of species trees from multilocus data. *Molecular Biology and Evolution* **27**, 570–580.

- Horton T, Kroh A, Ah Yong S, Bailly N, Boyko CB, Brandão SN, Gofas S, Hooper JNA, Hernandez F, Holovachov O, Mees J, Molodtsova TN, Paulay G, Decock W, Dekeyzer S, Poffyn G, Vandepitte L, Vanhoorne B, Adlard R, Agatha S, Ahn KJ, Akkari N, Alvarez B, Anderberg A, Anderson G, Angel MV, Antic D, Arango C, Artois T, Atkinson S, Auffenberg K, Baldwin BG, Bank R, Barber A, Barbosa JP, Bartsch I, Bellan-Santini D, Bergh N, Bernot J, Berta A, Bezerra TN, Bieler R, Blanco S, Blasco-Costa I, Blazewicz M, Bock P, Bonifacino de León M, Böttger-Schnack R, Bouchet P, Boury-Esnault N, Boxshall G, Bray R, Bruce NL, Cairns S, Calvo Casas J, Carballo JL, Cárdenas P, Carstens E, Chan BK, Chan TY, Cheng L, Churchill M, Coleman CO, Collins AG, Collins GE, Corbari L, Cordeiro R, Cornils A, Coste M, Costello MJ, Crandall KA, Cremonese F, Cribb T, Cutmore S, Dahdouh-Guebas F, Daly M, Daneliya M, Dauvin JC, Davie P, De Broyer C, De Grave S, de Mazancourt V, de Voogd NJ, Decker P, Decraemer W, Defaye D, d'Hondt JL, Dippenaar S, Dohrmann M, Dolan J, Domning D, Downey R, Ector L, Eisendle-Flöckner U, Eitel M, Encarnação SCd, Enghoff H, Epler J, Ewers-Saucedo C, Faber M, Figueroa D, Finn J, Fišer C, Fordyce E, Foster W, Frank JH, Franssen C, Freire S, Furuya H, Galea H, Gao T, Garcia-Alvarez O, Garcia-Jacas N, Garic R, Garnett S, Gasca R, Gaviria-Melo S, Gerken S, Gibson D, Gibson R, Gil J, Gittenberger A, Glasby C, Glover A, Gómez-Noguera SE, González-Solís D, Gordon D, Gostel M, Grabowski M, Gravili C, Guerra-García JM, Guidetti R, Guiry MD, Gutierrez D, Hadfield KA, Hajdu E, Hallermann J, Hayward BW, Heiden G, Hendrycks E, Herbert D, Herrera Bachiller A, Ho Js, Hodda M, Høeg J, Hoeksema B, Houart R, Hughes L, Hyžný M, Iniesta LFM, Iseto T, Ivanenko S, Iwataki M, Janssen R, Jarms G, Jaume D, Jazdzewski K, Jersabek CD, Józwiak P, Kabat A, Kantor Y, Karanovic I, Karthick B, Katinas L, Kim YH, King R, Kirk PM, Klautau M, Kociolek JP, Köhler F, Kolb J, Kotov A, Kremenetskaia A, Kristensen RM, Kulikovskiy M, Kullander S, Kupriyanova E, Lambert G, Lazarus D, Le Coze F, LeCroy S, Leduc D, Lefkowitz EJ, Lemaitre R, Lichter-Marck IH, Lindsay D, Liu Y, Loeuille B, Lörz AN, Lowry J, Ludwig T, Lundholm N, Macpherson E, Madin L, Mah C, Mamo B, Mamos T, Manconi R, Mapstone G, Marek PE, Marshall B, Marshall DJ, Martin P, Mast R, McFadden C, McInnes SJ, Meidla T, Meland K, Merrin KL, Messing C, Mills C, Moestrup Ø, Mokievsky V, Monniot F, Mooi R, Morandini AC, Moreira da Rocha R, Morrow C, Mortelmans J, Mortimer J, Musco L, Nesom G, Neubauer TA, Neubert E, Neuhaus B, Ng P, Nguyen AD, Nielsen C, Nishikawa T, Norenburg J, O'Hara T, Opresko D, Osawa M, Osigus HJ, Ota Y, Páll-Gergely B, Panero JL, Pasini E, Patterson D, Paxton H, Pelsler P, Peña-Santiago R, Perrier V, Perrin W, Petrescu I, Picton B, Pilger JF, Pisera AB, Polhemus D, Poore GC, Potapova M, Pugh P, Read G, Reich M, Reimer JD, Reip H, Reuscher M, Reynolds JW, Richling I, Rimet F, Ríos P, Rius M, Rodríguez E, Rogers DC, Roque N, Rosenberg G, Rützler K, Sabbe K, Saiz-Salinas J, Sala S, Santagata S, Santos S, Sar E, Satoh A, Saucède T, Schatz H, Schierwater B, Schilling E, Schmidt-Rhaesa A, Schneider S, Schönberg C, Schuchert P, Senna AR, Serejo C, Shaik S, Shamsi S, Sharma J, Shear WA, Shenkar N, Shinn A, Short M, Sicinski J, Sierwald P, Simmons E, Sinniger F, Sivell D, Sket B, Smit H, Smit N, Smol N, Souza-Filho JF, Spelda J, Sterrer W, Stienen E, Stoev P, Stöhr S, Strand M, Suárez-Morales E, Summers M, Suppan L, Susanna A, Suttle C, Swalla BJ, Taiti S, Tanaka M, Tandberg AH, Tang D, Tasker M, Taylor J, Taylor J, Tchesunov A, Temereva E, ten Hove H, ter Poorten JJ, Thomas JD, Thuesen EV, Thurston M, Thuy B, Timi JT, Timm T, Todaro A, Turon X, Tyler S, Uetz P, Urbatsch L, Uribe-Palomino J, Urtubey E, Utevsky S, Vacelet J, Vachard D, Vader W, Väinölä R, Van de Vijver B, van der Meij SE, van Haaren T, van Soest RW, Vanreusel A, Venekey V, Vinarski M, Vonk R, Vos C, Walker-Smith G, Walter TC, Watling L, Wayland M, Wesener T, Wetzel CE, Whippo C, White K, Wieneke U, Williams DM, Williams G, Wilson R, Witkowski A, Witkowski J, Wyatt N, Wylezich C, Xu K, Zanol J, Zeidler W and Zhao Z (2020) World Register of Marine Species. World Wide Web electronic publication. <https://www.marinespecies.org> (accessed 25 august 2020). <https://doi.org/10.14284/170>.
- Huelsenbeck JP and Ronquist F (2001) MrBayes: Bayesian inference of phylogenetic trees. *Bioinformatics (Oxford, England)* **17**, 754–755.
- Iannaccone JA, López EN and Alvarino LF (2000) *Procamallanus (Spirocamallanus) inopinatus* Travassos, Artigas et Pereira, 1928 (Nematoda: Camallanidae) parasito de *Triportheus angulatus* (Spix, 1829) (Characidae) en la laguna de Yarinacocha, Ucayali-Peru. *Biología Pesquera* **28**, 37–43.
- Jackson JA and Tinsle RC (1995) Representatives of *Batrachocamallanus* N. g. (Nematoda: Procamallaninae) from *Xenopus* Spp. (Anura: Pipidae): geographical distribution, host range and evolutionary relationships. *Systematic Parasitology* **31**, 159–188.
- Kimura M (1980) A simple method for estimating evolutionary rates of base substitutions through comparative studies of nucleotide sequences. *Journal of Molecular Evolution* **16**, 111–120.
- Kloss GR (1966) Helminthos parasitos de espécies simpátricas de *Astyanax* (Pisces, Characidae). *Papéis Avulsos do Departamento de Zoologia São Paulo* **18**, 189–219.
- Kohn A and Fernandes BMM (1987) Estudo comparativo dos helmintos parasitos de peixes do Rio Mogi Guassu, coletados nas excursões realizadas entre 1927 e 1985. *Memórias do Instituto Oswaldo Cruz* **82**, 483–500.
- Luque JL, Aguiar JC, Vieira FM, Gibson DI and Portes-Santos C (2011) Checklist of Nematoda associated with the fishes of Brazil. *Zootaxa* **3082**, 1–88.
- Luque JL, Cruces C, Chero J, Paschoal F, Alves PV, Da Silva AC, Sanchez L and Iannaccone J (2016) Checklist of metazoan parasites of fishes from Peru. *Check List (Luis Felipe Toledo)* **6**, 659–667.
- Moravec F (1998) *Nematodes of Freshwater Fishes of the Neotropical Region*. Praha: Academia.
- Moravec F and Jirků M (2015) Two *Procamallanus (Spirocamallanus)* species (Nematoda: Camallanidae) from freshwater fishes in lower Congo river. *Acta Parasitologica* **60**, 226–233.
- Moravec F and Justine, J-L. (2019) A new species and new records of camallanid nematodes (Nematoda, Camallanidae) from marine fishes and sea snakes in New Caledonia. *Parasite* **26**, 66.
- Moravec F and Thatcher VE (1997) *Procamallanus (Denticamallanus* Subgen. n.) *dentatus* sp. n. (Nematoda, Camallanidae) from the characid fish, *Bryconops Alburnoides*, in the Brazilian Amazon. *Parasite* **4**, 239–243.
- Moravec F, Kohn A and Fernandes BMM (1993) Nematode parasites of fishes of the Paraná River, Brazil. Part 3. Camallanoidea and Dracunculoidea. *Folia Parasitologica* **40**, 211–229.
- Moravec F, Prouza A and Royero R (1997) Some nematodes of freshwater fishes in Venezuela. *Folia Parasitologica* **44**, 33–47.
- Moravec F, Salgado-Maldonado G and Caspeta-Mandujano J (2000) Three new *Procamallanus (Spirocamallanus)* species from freshwater fishes in Mexico. *Journal of Parasitology* **86**, 119–127.
- Moravec F, Justine, J-L, Würtz J, Tarachewski H and Sasal P (2006) A new species of *Procamallanus* (Nematoda: Camallanidae) from Pacific eels (*Anguilla* Spp.). *Journal of Parasitology* **92**, 130–137.
- Moreira NIB., Oliveira CL and Costa HMA (1994) *Spirocamallanus inopinatus* (Travassos, Artigas & Pereira, 1928) e *Spirocamallanus Saofranciscensis* sp. n. (Nematoda, Camallanidae) em peixes da Represa de Tres Maria. *Arquivo Brasileiro de Medicina Veterinária e Zootecnia* **46**, 485–500.
- Nichols R (2001) Gene trees and species trees are not the same. *Trends in Ecology and Evolution* **16**, 358–364.
- Notredame C, Higgins DG and Heringa J (2000) T-Coffee: a novel method for fast and accurate multiple sequence alignment. *Journal of Molecular Biology* **302**, 205–217.
- Pereira C (1935) Ascaridata e spirurata parasitos de peixes do Nordeste Brasileiro. *Arquivos do Instituto Biológico São Paulo* **6**, 53–62.
- Petter AJ and Dlouhy C (1985) Nématodes de Poissons du Paraguay. III. Camallanina. Description d'une espèce et d'une sous-espèce nouvelles de la famille des Guyanemidae. *Revue Suisse de Zoologie* **92**, 165–175.
- Petter AJ and Thatcher VE (1988) Observations sur la structure de la capsule buccale de *Spirocamallanus inopinatus* (Nematoda), parasite de poissons brésiliens. *Bulletin du Museum National d'Histoire Naturelle* **10**, 685–692.
- Pinheiro RH da S, Melo FTV, Monks S, dos Santos, JN and Giese EG (2018) A new species of *Procamallanus* Baylis, 1923 (Nematoda, camallanidae) from *Astronotus ocellatus* (Agassiz, 1831) (Perciformes, Cichlidae) in Brazil. *Zookeys* **790**, 21–33.
- Pons J, Barraclough TG, Gomez-Zurita J, Cardoso A, Duran DP, Hazell S, Kamoun S, Sullin WD and Vogler AP (2006) Sequence-based species delimitation for the DNA taxonomy of undescribed insects. *Systematic Biology* **55**, 595–609.
- Puillandre N, Lambert A, Brouillet S and Achaz G (2012) ABGD, automatic barcode Gap discovery for primary species delimitation. *Molecular Ecology* **21**, 1864–1877.

- Rambaut A, Drummond AJ, Xie D, Baele G and Suchard MA (2018) Posterior summarization in Bayesian phylogenetics using tracer 1.7. *Systematic Biology* **67**, 901–904. <https://doi.org/10.1093/sysbio/syy032>.
- Razkin O, Sonet G, Breugelmans K, Madeira MJ, Gómez-Moliner BJ and Backeljau T (2016) Species limits, interspecific hybridization and phylogeny in the cryptic land snail complex *Pyramidula*: the power of RADseq data. *Molecular Phylogenetics and Evolution* **101**, 267–278.
- Reis RE, Albert JS, Di Dario F, Mincarones MM, Petry P and Rocha LA (2016) Fish biodiversity and conservation in South America. *Journal of Fish Biology* **89**, 12–47.
- Sardella CJ, Pereira FB and Luque JL (2017) Redescription and first genetic characterisation of *Procamallanus (Spirocamallanus) Macaensis* Vicente & Santos, 1972 (Nematoda: Camallanidae), including re-evaluation of the species of *Procamallanus (Spirocamallanus)* from marine fishes off Brazil. *Systematic Parasitology* **94**, 657–668.
- Svitin R, Schoeman AL and du Preez L.H. (2018) New information on morphology and molecular data of camallanid nematodes parasitising *Xenopus laevis* (Anura: pipidae) in South Africa. *Folia Parasitologica* **65**, 003.
- Svitin R, Truter M, Kudlai O, Smit NJ and du Preez L. (2019) Novel information on the morphology, phylogeny and distribution of camallanid nematodes from marine and freshwater hosts in South Africa, including the description of *Camallanus Sodwanaensis* n. sp. *International Journal for Parasitology: Parasites and Wildlife* **10**, 263–273.
- Townsend JP (2007) Profiling phylogenetic informativeness. *Systematic Biology* **56**, 222–231.
- Travassos L, Artigas P and Pereira C (1928) Fauna helmintológica dos peixes de água doce do Brasil. *Arquivos do Instituto Biológico* **1**, 5–68.
- Uetz P, Freed P and Hosek J (eds) (2020) The Reptile Database. World Wide Web electronic publication. <http://www.reptile-database.org> (accessed 25 May 2020).
- Vicentin W, Vieira KRI, Tavares LER., Costa FE, Takemoto RM and Paiva F (2013) Metazoan endoparasites of *Pygocentrus Nattereri* (Characiformes: Serrasalminae) in the Negro river, Pantanal, Brazil. *Revista Brasileira de Parasitologia Veterinária* **22**, 331–338.
- Wijová M, Moravec F, Horák A and Lukeš J (2006) Evolutionary relationships of *Spirurina* (Nematoda: Chromadorea: Rhabditida) with special emphasis on dracunculoid nematodes inferred from SSU rRNA gene sequences. *International Journal for Parasitology* **36**, 1067–1075.
- Xia X (2018) DAMBE 7: new and improved tools for data analysis in molecular biology and evolution. *Molecular Biology and Evolution* **35**, 1550–1552.
- Xia X, Xie Z and Li WH (2003) Effects of GC content and mutational pressure on the lengths of exons and coding sequences. *Journal of Molecular Evolution* **56**, 362–370.
- Zar JH (2010) *Biostatistical Analysis*. Englewood Cliffs: Prentice Hall.
- Zhang J, Kapli P, Pavlidis P and Stamatakis A (2013) A general species delimitation method with applications to phylogenetic placements. *Bioinformatics (Oxford, England)* **29**, 2869–2876.